

The Low-lying Excitations of Polydiacetylene

A. Race ¹, W. Barford ¹ and R. J. Bursill ²

¹*Department of Physics and Astronomy, The University of Sheffield, Sheffield, S3 7RH, United Kingdom.*

²*School of Physics, The University of New South Wales, Sydney, NSW 2052, Australia.*

Abstract

The Pariser-Parr-Pople Hamiltonian is used to calculate and identify the nature of the low-lying vertical transition energies of polydiacetylene. The model is solved using the density matrix renormalisation group method for a fixed acetylenic geometry for chains of up to 102 atoms. The non-linear optical properties of polydiacetylene are considered, which are determined by the third-order susceptibility. The experimental $1B_u$ data of Giesa and Schultz are used as the geometric model for the calculation. For short chains, the calculated $E(1B_u)$ agrees with the experimental value, within solvation effects (~ 0.3 eV). The charge gap is used to characterise bound and unbound states. The nB_u is above the charge gap and hence a continuum state; the $1B_u$, $2A_g$ and mA_g are not and hence are bound excitons. For large chain lengths, the nB_u tends towards the charge gap as expected, strongly suggesting that the nB_u is the conduction band edge. The conduction band edge for PDA is agreed in the literature to be ~ 3.0 eV. Accounting for the strong polarisation effects of the medium and polaron formation gives our calculated $E_\infty(nB_u) \sim 3.6$ eV, with an exciton binding energy of ~ 1.0 eV. The $2A_g$ state is found to be above the $1B_u$, which does not

agree with relaxed transition experimental data. However, this could be resolved by including explicit lattice relaxation in the Pariser-Parr-Pople-Peierls model. Particle-hole separation data further suggest that the $1B_u$, $2A_g$ and mA_g are bound excitons, and that the nB_u is an unbound exciton.

I INTRODUCTION

Polymers, and other molecular materials, that exhibit non-linear optical properties and electroluminescence have attracted much interest amongst theorists and experimentalists, owing to their possible use in organic technology [1]–[7]. Poly(diacetylene)s (PDAs) with the general formula shown in Fig. 1. (a) are the π -conjugated organic polymers studied here: they exhibit non-linear optical properties, near-perfect crystal structure and doping-dependent transport properties. These properties make them ideally suited for use in the theorist’s calculation. A full characterisation of PDA’s electronic properties would mean a better understanding of π -conjugated polymers in general. In PDA with a very low polymer content ($x_p < 10^{-3}$ in weight), interchain interaction is minimal and thus it can be considered an ideal one-dimensional model system.

There have been many calculations performed on PDA with varying degrees of success. Parry conducted a SCF calculation and found an energy gap that was too low [8]. Boudreaux’s SCF- $X\alpha$ calculation gives an energy gap of 2.21 eV, which agrees well with the long-chain experimental extrapolations for the energy gap of 2.11 eV and 2.25 eV (yellow phase) [9]–[10]. A further SCF- $X\alpha$ calculation by Boudreaux [11] accounts for charge density

waves by the same geometric Hückel model of Whangbo [12]. The *ab initio* crystal orbital calculations of Kertesz give energy gaps that are too high [13]–[14]. Predicted bond lengths show impressive agreement with x-ray data in Karpfen’s *ab initio* SCF calculation [15]. He performed a total energy minimisation to calculate bond lengths and shows that the energy difference between butatriene and acetylene structure per unit cell is 0.52 eV. This agrees with previous calculations and experiment [12, 16]. A similar calculation yielding similar results was performed by Brédas [17].

Wilson, Cojan, Cade and Movaghar [18]–[20] performed Hückel band structure calculations for the infinitely long PDA chain. Cajon and Wilson did not include bond alteration in their calculation, and thus modelled a compound with one distinct chemical bond. The energy gap was found to be too low. Cade and Movaghar used two degrees of freedom in their calculation as a bond alteration parameter.

Extended Hückel calculations have been performed by Parry and Whangbo [12, 21]. The work of Parry is restricted to one distinct chemical structure and, as with other parameterisations, yields a value for the energy gap that is too low. The model employed by Wangbo has a hopping term of the form:

$$t = t_0(1 \pm \delta) \tag{1}$$

with $0 < \delta < 1$. This produces results that are, again, quantitatively too low; however, it does generate an energy difference of 0.48 eV between the butatriene and acetylene structures, in excellent agreement with other calculations and experiment [15]–[16]. In summary, therefore, all these models are seen to give good qualitative predictions for bond alteration, but the

data are seen to be consistently red-shifted owing to their single particle picture.

The importance of screening in PDA is still considered controversial to many authors, because it determines the role of electron-electron correlations. A simple way to account for screening is to adjust the single chain electron-electron interaction potential $V(r)$, a method suggested by many authors. For example, Abe lowered the Hubbard parameter U from 11 to 5 eV and used a large long-range dielectric constant in a Ohno potential [22]–[23]. However, this again causes red-shifted energy gaps and results in unphysical atomic cohesion energies. We emphasise that there is clear and indisputable evidence that electron-electron interactions are of paramount importance in the electronic structure calculations of PDA. First, in polymeric crystal form, the linear absorption spectrum is seen to be symmetric and peaks at ~ 1.8 - 1.9 eV. However, the onset of photoconduction occurs not at this value but at ~ 2.3 - 3.0 eV (corresponding to uncorrelated π - π^* transitions) [24]. In addition, comparison of the linear absorption with the EA spectrum shows an EA feature at ~ 2.0 eV corresponding to the first derivative of the absorption: this is attributed to the Stark shift of the exciton. There is also an oscillating Franz-Keldysh band-edge structure at ~ 2.5 - 3.0 eV, with a lineshape that deviates from the first derivative of the absorption. The oscillations are due to interband transitions and coincide with the onset of photoconduction. These data independently suggest that the exciton binding energy is ~ 0.5 eV [25]–[27]. We note that these values show a great deal of variability owing to the variety of phases and the disorder present in PDA. Hence, despite the apparent success of the Su-Schrieffer-Heeger model [28]–[29] neutral excitons with large binding energies are the low-lying excitations in

PDA [24], [30]–[31]. This is borne out by the Pariser-Parr-Pople calculation presented in this work, which incorporates electron-electron interactions.

II MODELLING POLYDIACETYLENE

A Electronic Structure

The atomic orbital model used in the calculation is described as follows. Carbon has the atomic configuration $1s^2 2s^2 2p^2$. Since carbon has four valence electrons, there is an alternating structure of two sp^2 and two sp hybridised carbon atoms that can account for the idealised PDA chemical composition. (See Fig. 1.)

Since PDA is spatially centrosymmetric, and thus shows C_2 symmetry, the wavefunctions possess mirror plane and centro-inversion symmetries. The group notation for mirror plane symmetries are A for the symmetric and B for the antisymmetric case. Inversion symmetries are labelled g for symmetric and u for antisymmetric. The ground state is therefore labelled $1A_g$ and the first optically active dipole from the ground state has to be the $1B_u$ state. The wavefunctions are either even (A_g) or odd (B_u) under an inversion.

B Geometric Structure

Although there is a myriad of literature on the optical properties of PDA, there is still little on their structural and conformational properties, which prevents extensive theoretical

investigation. The work of Giesa and Schultz [10] following that of Wudl and Bitler [32] describes the synthesis and thorough characterisation of the series of alternating all-*trans*-polyenyne without substituents at the vinylic bonds that are studied in this paper.

To maintain consistency with the literature, the unsubstituted model compounds are named as follows:

$$C_n[N] \tag{2}$$

where the number of unsaturated carbon atoms n specifies each compound, and the number of formal monomer units N are added in the square brackets for clarity. The relation between n and N is,

$$n = 2(2N + 1). \tag{3}$$

These structures are shown in Fig. 2. In contrast with the simplest conjugated polymer represented by *trans*-polyacetylene, the carbon backbone of PDA contains two, additional, localized π electrons in every unit cell. Thus, there are two possibilities of bond alternation in this system that lead to non-equivalent structures with non-degenerate ground states, as shown in Fig. 1. (b) and (c). Work on the molecular geometries of C_{14} [3] and C_{22} [5] by X-ray structure analysis has determined bond lengths and angles that represent a typical *acetylene* structure (see TABLE I.) and no evidence for a *butatriene* form is found. In addition, Giesa shows that substitution does not alter the polymer structure significantly. Increasing the

size of the polymer does elongate double and triple bonds, while reducing the single bond; however, this is not pronounced. Hence, overall, these findings justify the use of the model acetylene structure employed in this paper, because an increase in conjugation length does not show a substantial effect on bond lengths and angles. Hence, owing to PDA's simple electronic and geometric ground-state structure, the Pariser-Parr-Pople Hamiltonian can easily describe it.

III THE PARISER-PARR-POPLE HAMILTONIAN

The Pariser-Parr-Pople Hamiltonian is:

$$\begin{aligned} \hat{H}_{PPP} = & - \sum_{\langle ij \rangle > \sigma} t_{ij} (c_{i\sigma}^\dagger c_{j\sigma} + c_{j\sigma}^\dagger c_{i\sigma}) + U \sum_i (n_{i\uparrow} - \frac{1}{2})(n_i - \frac{1}{2}) \\ & + \sum_{\substack{i \neq j \\ \sigma \sigma'}} V_{ij} (n_{i\sigma} - 1)(n_{j\sigma'} - 1) \end{aligned} \quad (4)$$

where the operator $c_{i\sigma}^\dagger (c_{i\sigma})$ creates (annihilates) a $2p_z$ electron of spin σ at site i (the i th carbon atom), $t_{i,j}$ (>0) is the transfer integral between the nearest neighbour atomic orbitals. The first term in the Hamiltonian allows the electrons to “hop” from one atom to another, and represents the kinetic energy gained from delocalising an electron from its atomic site. $n_{i\sigma} = c_{i\sigma}^\dagger c_{i\sigma}$ is the number density operator, and $\langle ij \rangle$ denotes nearest neighbours. U is the Pariser-Parr-Pople Coulomb repulsion between two electrons occupying the same $2p_z$ orbital and $U = 10.06$ eV [36]. V_{ij} is the long-range Coulomb repulsion and, in this work, is the Ohno function, $V_{ij} = U/\sqrt{1 + \beta r_{ij}^2}$ where $\beta = (U/14.397)^2$ and r_{ij} is the interatomic distances measured in Å [37].

The general expression for the resonance integrals is given by:

$$t_{ij} = t_0 + \alpha(r_{ij} - r_0) \quad (5)$$

where α is the coupling constant of electron-phonon interactions, r_{ij} is the length of the bond between carbon atoms i and j , and r_0 is the average bond length of the reference system.

The parameters in expression (4) are derived using polyacetylene as a reference system. First, it is pertinent to consider the gradient of the resonance integral with respect to bond length. It has been shown that the difference δt of the resonance integral is 0.2162 eV and the corresponding average change in bond lengths δl is 0.0471 [39]. Thus, the electron-phonon coupling constant is:

$$\alpha = \frac{\delta t}{\delta l} = \frac{0.2162}{0.0471} \text{ eV} \quad (6)$$

A full list of Hamiltonian parameters derived from polyacetylene used in this work is shown in TABLE II., and a schematic of the unit cell is found in Fig. 3.

The different resonance integrals are determined by the specific structures of the chain with lattice constant $4a$. Perturbations of the equidistant carbon chain lead to the energy gaps E_g and E'_g . The ground state corresponds to a fully filled valence band and unoccupied conduction band. The $1B_u$ is reached from the ground state by exciting one electron from the highest occupied molecular orbital (HOMO) to the lowest unoccupied molecular orbital (LUMO) (see Fig. 4.).

Although this band picture is useful in identifying important states, it has been shown that interactions *do* play an important part in the physics of PDA, as mentioned earlier.

By including the on-site and long range terms explicitly in the Hamiltonian (4) electron-electron interactions are taken into account, giving an accurate treatment of the electronic structure of PDA. Turning on the interactions, U and V_{ij} , changes the relative position of electronic states and can even cause the crossing of states. This non-interacting picture is therefore modified and an excitonic picture formulated. An electron and hole can bind together by their Coulomb field to produce an exciton, or bound electron-hole pair. Since the conduction band signifies the non-interacting limit, excitons are energetically situated below the conduction band.

IV RESULTS AND DISCUSSION

A Essential States

Non-linear optical experimental data can be used to characterise the low-lying states of π -conjugated polymers. The relative ordering of these states can elucidate much of the physics of such systems [30], [40]–[42]. Non-linear optical processes in polymers with C_2 symmetry are determined by the third-order susceptibility, $\chi^3(-\omega_1 - \omega_2 - \omega_3; \omega_1, \omega_2, \omega_3)$, which is calculated by the sum over all available states. This makes calculating $\chi^{(3)}$ in principle difficult, owing to the large number of paths included. However, it is found that there are certain *essential states* that are important when considering the $\chi^{(3)}$ of π -conjugated polymers, as only the essential states make a significant contribution to it. The four essential states are the ground state, the first odd-parity exciton state, $1B_u$, the charge transfer state, mA_g , and the nB_u (see Fig.

5.). Another important state is the $2A_g$: this is a two-photon state, whose position relative to the $1B_u$ determines whether a polymer exhibits photoluminescence. The importance of these states is the result of the strong and dominant dipole couplings amongst them in

$$\mu_{if} = \langle f | \hat{\mu} | i \rangle \quad (7)$$

resulting in their substantial contribution to non-linear optical spectroscopy. Hence, an important first step in identifying the non-linear properties of PDA is calculating the dipole moments of transitions between states. As the DMRG method is a robust and accurate method of finding dipole moments the essential states can be found. These are given in TABLE III. However, they are only calculated for polymers of up to 26 sites. This is because the important optical states become interlaced with other states of a spin-density-wave character (i.e., those related to the $2A_g$). Since we can only target approximately 10 states in each symmetry sector, the mA_g and the nB_u states soon become impossible to track.

An analysis of the essential states and the $2A_g$ forms the remainder of this discussion. They are paramount when considering the physics of π -conjugated polymers, as mentioned above, and are compared with experimental data. In Section IV (B) the vertical excitation energies of the essential states and the $2A_g$ are analysed. Section IV (C) contains particle-hole separation data, which is used to confirm predictions made in Section IV (B) and help identify the nature of the $1B_u$, $2A_g$, nB_u and mA_g states.

B Vertical Excitation Energies

The DMRG method, used by Barford and Bursill [7], following the work of White [43], was implemented on the model system to find the vertical low-lying energy eigenvalues of PDA. The low-lying excitations are bound particle-hole pairs, which behave as composite particles. These particles delocalise along the polymer backbone as effective single particles, and thus their dispersion should be characteristic of single particles. In PDA the excitons effectively tunnel between double and triple bond dimers. In an effective particle model, this would be modelled as a linear chain, with two ‘sites’ per unit cell. The dispersion should scale as $1/n^2$, as these are states *within* the exciton band. In contrast, the band gap is associated with free, single particle transitions across the HOMO-LUMO gap. An examination of the dispersion relation of Lennard-Jones [44] indicates that this energy should scale as $1/n$ in the asymptotic limit. However, neither a solely $1/n$ nor $1/n^2$ fit for the free particle-hole and exciton dispersions, respectively, is accurate for small chains, owing to higher-order corrections, and the fit required cannot be used to characterise states. In this work, therefore, a polynomial fit is preferred for extrapolating the data.

The calculated vertical excitation energies for the $1B_u$, $2A_g$, mA_g , nB_u and charge gap, Δ , are plotted in Fig. 6. against $1/n$. In addition, the polynomial extrapolations for the long-chain limit are shown in TABLE IV. for some of the states. The charge gap is a useful criterion for characterising excitonic and unbound states, and is given as follows,

$$\Delta = E(n + 1) + E(n - 1) - 2E(n) \quad (8)$$

Here $E(n)$ is the ground-state energy of the n electron system. The charge gap signifies the lowest energy excitation of an electron from the valence to conduction band. Thus states above Δ are unbound excitons; those below it are bound. Of the states plotted in Fig. 6. only the nB_u is positioned above the charge gap, suggesting that the nB_u is a continuum state. Conversely, the $1B_u$, $2A_g$ and mA_g , are below it and are thus bound excitons. This is shown to be true in Section IV (C) by examining the particle-hole separation of these states.

The experimental data obtained by Giesa [10] are also plotted in Fig. 6. A polynomial extrapolation of the experimental data yields $E_\infty \sim 2.5$ eV; however, this is considered unreliable as there are so few points used in the fit. For short chains the calculated and experimental $1B_u$ energies are remarkably within solvation (polarisation) effects of the experimental medium (~ 0.3 eV). This solvation value is derived from the work of Yaron, who predicts 0.3 eV for the $1B_u$ [23]. In addition, Barford and Bursill's calculation on polyenes [39] found $E(1B_u)$ to be 0.3 eV above the experimental value. Their recent calculations on PPP and PPV yield similar results [45]. Our calculated $E_\infty(1B_u)$ for PDA is ~ 3.0 eV, and, hence, correcting for solvation effects gives our calculated $E_\infty(1B_u) \sim 2.7$ eV.

The energy of the nB_u is seen to tend to that of the charge gap for $n \rightarrow \infty$, as seen in Fig. 6. Hence, the extrapolated long chain nB_u energy is found to be ~ 5.7 eV, and this state is predicted to be the conduction band threshold. However, the onset of photoconduction (continuum limit) is ~ 3.0 eV. The large polarisation effects of the surrounding medium can correct for this: these are estimated by Yaron to be ~ 1.5 eV [23]. In addition, polaron formation means a further $\sim 2 \times 0.3$ eV can be subtracted from 5.7 eV [39]. Including all

these effects gives $E_\infty(nB_u) \sim 3.6$ eV, which is in reasonable agreement with the experimental conduction band threshold quoted earlier. Therefore, the exciton binding energy is $E_b = E_\infty(nB_u) - E_\infty(1B_u)$, and from our calculation is found to be $3.6 - 2.7 \sim 0.9$ eV. This is in reasonable agreement with binding energies found in the literature [25]–[27].

Having identified the important non-linear optical states in PDA from the dipole moments, and calculated the corresponding excitation energies, an energy level diagram can be drawn. This is shown for 26 atoms in Fig.7. As expected there is a large $1A_g \rightarrow 1B_u$ dipole moment, corresponding to the one-photon absorption, while the band threshold (nB_u) has a weak coupling to the ground state. It is seen that the first excited A_g state is above the $1B_u$, which would suggest that PDA shows photoluminescence. (There is a direct $1A_g \rightarrow 1B_u$ transition.) However, experiments have shown that PDA is not electro-luminescent: measurements of the frequency dependence of third harmonic generation in Langmuir-Blodgett films of PDA indicate that an A_g singlet state is ~ 0.11 eV below the lowest energy B_u state. In addition, the recent work of Kohler and Schilke [46] has shown an A_g symmetry state ~ 0.21 eV lower than the lowest B_u symmetry state. Our model calculates vertical transitions only and is seen to agree with many theoretical vertical-energy calculations of PDA. Singlet exciton relaxation studies on isolated polydiacetylene chains by subpicosecond pump-probe experiments have suggested that nonradiative singlet B_u exciton relaxation involves two A_g states in series [47]. As it is well known that electron-phonon coupling is strong in PDA, we propose that lattice relaxation effects produce these A_g states. It is hoped that this will be resolved by studies of lattice relaxation explicitly within the Pariser-Parr-Pople-Peierls

Hamiltonian, which are now in progress. Similar studies by Barford on polyenes have found that the relaxation energies of the $1B_u$ and $2A_g$ can be reduced by as much as 0.3 and 1.0 eV, respectively [48]–[49]. Thus, including lattice relaxation in the Pariser-Parr-Pople-Peierls model is expected to bring the $2A_g$ state below the $1B_u$ in agreement with experiment.

C Particle-hole Separation

In order to help characterise the low-lying A_g and B_u states the particle-hole separation is calculated and gives an indication of the spatial extent of a given state: an explanation of how it is calculated is given in the Appendix. Suffice it here to say that we use the one-particle singlet excitation correlation function, which directly relates a hole in the valence band to an electron in the conduction band. In essence, if a particular state’s particle-hole separation is seen to increase with system size, the electron and hole are unbound. However, if this quantity reaches a maximum, the Coulomb attraction between the electron and hole is strong enough to bind them together. In Fig. 8. the particle-hole separations are given as a function of system size in units of the average C-C bond length for the $1B_u$, $2A_g$ and mA_g states. It is clear that the $1B_u$, $2A_g$ and mA_g states are all bound excitons because the electron-hole separation reaches a maximum value with increasing chain length. These signify the composite particles mentioned in Section IV (B). However, the particle-hole separation of the nB_u state increases linearly with system size: this suggests that the nB_u is either very weakly bound or unbound. We conclude therefore that for PDA molecules of up to 26 carbon atoms the electron-hole continuum (i.e., the band edge) is expected to be the

nB_u , further strengthening the arguments of Section IV (B).

V CONCLUSIONS

The DMRG calculation of a suitably parameterised Pariser-Parr-Pople Hamiltonian for a *rigid geometry* can be used to describe the electronic structure of short or long chain polydiacetylene polymers. The role of electron-electron interactions is fundamental in the low-lying excitations, and this is borne out in our calculation. We have found and characterised the essential states: these are the $1A_g$, $1B_u$, mA_g and nB_u . Our $1B_u$ excitation energies are within a few tenths of an eV of the experimental ones: for short chains, the calculated $E(1B_u)$ agrees with the experimental value, within solvation effects (~ 0.3 eV). The nB_u is found to be above the charge gap, and hence it is continuum state; the $1B_u$, $2A_g$ and mA_g are not, and hence are bound excitons. For large chain lengths the nB_u tends towards the charge gap as expected, strongly suggesting that the nB_u is the conduction band edge. We found our calculated conduction band edge to agree reasonably with the experimental value of ~ 3.0 eV quoted in the literature. Accounting for the strong polarisation effects of the medium and polaron formation gives our calculated $E_\infty(nB_u) \sim 3.6$ eV, with an exciton binding energy of ~ 1.0 eV. Our $2A_g$ is calculated to be above the $1B_u$, which does not agree with relaxed-transition experiments: it is hoped that electron-lattice relaxation will adjust the position of the $2A_g$ to correct for this. Particle-hole separation data were used to help characterise the low-lying excitation in PDA. These data further suggest that the $1B_u$, $2A_g$ and mA_g are bound excitons, and that, conversely, the nB_u is an unbound exciton.

This work is further evidence that the essential states mechanism is adequate for describing the electronic properties of model π -conjugated polymers. Future work will include, as already discussed, the incorporation of electron-lattice relaxation, and a more thorough treatment of the triple bond using a ZINDO Hamiltonian.

ACKNOWLEDGEMENTS

We thank David Yaron for discussions. One of the authors (A. R.) is supported by the EPSRC (UK). The calculations were performed on the DEC8400 at the Rutherford Appleton Laboratory.

APPENDIX

To measure the particle-hole separation we use the particle-hole correlation function, introduced in Refs. [48] and [49]. Underlying this approach is the assumption that a particle-hole pair corresponds to the promotion of an electron from the valence (or HOMO) band to the conduction (or LUMO) band.

Without loss of generality, the atomic basis can be transformed to a local molecular orbital basis. The local molecular orbitals correspond to the bonding ($|1\rangle$) and anti-bonding ($|2\rangle$) combinations of the atomic orbitals on each dimer, where a dimer is a double or triple bond. The local molecular orbitals delocalise via the single bonds. Then, the creation operator,

$$S_{ij}^\dagger = \frac{1}{\sqrt{2}} \left(a_{i2\uparrow}^\dagger a_{j1\uparrow} + a_{i2\downarrow}^\dagger a_{j1\downarrow} \right) \quad (\text{A1})$$

promotes an electron from $|1\rangle$ on dimer j . to $|2\rangle$ on dimer i . However, since the local molecular orbitals are not exact Bloch transforms of the band molecular orbital¹ it is also necessary to include the hermitian conjugate of S_{ij} .

We now define the exciton correlation function with respect to the ground state, as:

$$C_{ij}^s(|n\rangle) = \langle n | (S_{ij}^\dagger + S_{ij}) | 1^1 A_g^+ \rangle \quad (\text{A2})$$

and the mean square of the particle-hole separation is:

$$\langle (i - j)^2 \rangle = \frac{\sum_{ij} (i - j)^2 (C_{ij}^s)^2}{\sum_{ij} (C_s^s)^2} \quad (\text{A3})$$

In practice, we do not consider all combinations of i and j , but restrict ourselves to i and j symmetrically spaced around the middle dimer.

¹ The exact Bloch transforms of the band molecular orbitals are Wannier molecular orbitals. The Wannier orbitals of the valence band are predominately $|1\rangle$, with a small admixture of $|2\rangle$ from neighbouring dimers.

References

- [1] J. M. Leng, S. Jeglinski, X. Wei, R. E. Benner, Z. V. Vardeny, F. Guo, S. Mazumdar, Phys. Rev. Lett. 72 156 (1994).
- [2] S. Heun, R. F. Mahrt, A. Greiner, U. Lemmer, H. Bessle, D. A. Halliday, D. D. C. Bradley, P. L. Burn, A. B. Holmes, J. Phys. C 5 247 (1993).
- [3] J. Cornil, D. Beljonne, R. H. Friend, J. L. Brédas, Chem. Phys. Lett 223 82-88 (1994).
- [4] M. Chandros, S. Mazumdar, S. Jeglinski, X. Wei, Z. V. Vardeny, E. W. Kwock, T. M. Miller, Phys. Rev. B 50 14702 (1994).
- [5] M. J. Rice, Yu N. Garstein, Phys. Rev. Lett. 73 2504 (1994).
- [6] Yu. N. Garstein, M. J. Rice, E. M. Conwell, Phys. Rev. Rev. B. 52 1683 (1995).
- [7] W. Barford, R. J. Bursill, Chem. Phys. Lett. 268 535 (1997).
- [8] D. E. Parry, Chem. Phys. Lett. 46 605 (1997).
- [9] H. Gross, H. Sixl, Mol. Cryst. Liq. Cryst. 93 261 (1983); H. Gross, Dissertation, Universität Stuttgart, 1984.
- [10] R. Giesa and R. C. Schultz, Polymer International 33 43-60 (1994).
- [11] D. S. Bourdreaux and R. R. Chance, Chem. Phys. Lett. 51 273 (1977).
- [12] M. -H. Whangbo, R. Hoffman, and R. B. Woodward, Proc. R. Soc. London Ser. A 366 23 (1979).

- [13] M. Kertesz, J. Koller, and A. Azman, *Chem. Phys.* 27, 273 (1978).
- [14] M. Kertesz, J. Koller, and A. Azman, *Chem. Phys. Lett.* 56, 18 (1978).
- [15] A. Karpfen, *J. Phys. C* 13 5673 (1980).
- [16] H. Sixl, W. Neumann, R. Huber, V. Denner, and E. Sigmund, *Phys. Rev. B* 31 142 (1985).
- [17] J. L. Brédas, M. Dory, and J. M. Andre, *J. Chem. Phys.* 83 5242 (1985).
- [18] E. G. Wilson, *J. Phys. C* 8 727 (1975).
- [19] C. Cojan, G. P. Agrawal, and C. Flytzanis, *Phys. Rev. B* 15 909 (1977).
- [20] N. A. Cade and B. Movaghar, *J. Phys. C* 16 539 (1983).
- [21] D. E. Parry, *Chem. Phys. Lett.* 43 597 (1976).
- [22] S. Abe, M. Schrieber, W. P. Su, and J. Yu, *J. Lumin.* 53 519 (1992).
- [23] E. Moore, B. Gherman, and D. Yaron, *J. Chem. Phys.* 106 10 (1997).
- [24] K. C. Yee and R. R. Chance, *J. Polym. Sci., Polym. Phys. Ed.* 16 431 (1978).
- [25] L. Sebastian and G. Weiser, *Phys. Rev. Lett.* 46 1156 (1981).
- [26] Y. Tokura, T. Koda, A. Itsubo, M. Myabayashi, K. Okuhara, and A. Ueda, *J. Chem. Phys.* 85 99 (1984).

- [27] T. Hasegawa, K. Ishikawa, T. Koda, K. Takeda, H. Kobayashi, and K. Kubodera, *Synth. Met.* 41-43 3151 (1991).
- [28] W. P. Su, J. R. Schrieffer, and A. J. Heeger, *Phys. Rev. Lett.* 42 1698 (1979).
- [29] W. P. Su, J. R. Schrieffer, and A. J. Heeger, *Phys. Rev. B* 22 2099 (1980).
- [30] D. Guo, S. Mazumdar, S. N. Dixit, F. Kajzar, F. Jarka, Y. Kawabe, and N. Peyghambarian, *Phys. Rev. B* 48 1433 (1993).
- [31] D. Moses, M. Sinclair, and A. J. Heeger, *Phys. Rev. Lett.* 58 2710 (1987).
- [32] F. Wudl, and S. P. Bitler, *J. Am. Chem. Soc.* 108 4685 (1986).
- [33] W. Neumann and H. Sixl, *Chem. Phys.* 58 303 (1981).
- [34] R. A. Huber, M. Schwoerer, H. Benk, and H. Sixl, *Chem. Phys. Lett.* 78 416 (1981).
- [35] C. Kollmar and H. Sixl, *J. Chem. Phys.* 88 2 (1988).
- [36] R. J. Bursill, R. J. Castleton, and W. Barford, *Chem. Phys. Lett.* 294 305 (1998).
- [37] K. Ohno, *Theor. Chem. Acta* 2 209 (1964).
- [38] L. Salem, *The Molecular Orbital Theory of Conjugated Systems* (Allyn and Bacon. Boston, 1973).
- [39] R. J. Bursill and W. Barford, *Phys. Rev. Lett.* 82 1514 (1999), W. Barford, R. J. Bursill and M. Yu Lavrentiev, unpublished.

- [40] F. Guo, Dandan, S. Mazumdar, S. N. Dixit, Synth. Metals. 49 1 (1992).
- [41] F. Guo, Dandan, S. Mazumdar, G. I. Stegeman, M. Cha D. Neher, S. Aramaki, W. Torruellas, and R. Zannoni, *Electrical, Optical, and Magnetic Properties of Organic Solid State Materials* 151 (1992).
- [42] F. Guo, Dandan, S. Mazumdar, S. N. Dixit, J. Nonlinear Optics (1992).
- [43] S. R. White, Phys. Rev. Lett. 69 2863(1992); Phys. Rev. B 48 10345 (1993).
- [44] J. E. Lennard-Jones, Proc. Roy. Soc A 158, 280 I (1937).
- [45] W. Barford and R. J. Bursill, unpublished.
- [46] B. E. Kohler, and D. E. Schilke, J. Chem. Phys. 86 9 (1987).
- [47] B. Kraabel and M. Joffre, Phys. Rev. B 58 23, 15777 (1998).
- [48] W. Barford, R. J. Bursill and M. Y. Lavrentiev, J. Phys.: Condens. Matter 10, 6429 (1988).
- [49] M. Y. Lavrentiev and W. Barford, Phys. Rev. B59, 15048 (1999).

FIGURES

FIG. 1. Chemical structure of a diacetylene trimer molecule. (a) Schematic representation of the orbitals giving rise to the different structures. The shaded orbitals give rise to σ -bonds, while the unshaded orbitals contain π -electrons in $2p$ orbitals. The $2p_z$ orbitals all overlap along the length. The molecular plane is in the x - y plane. (b) Acetylene structure. (c) Butatriene structure.

FIG. 2. The idealised chemical structure of the series of PDAs used in this work. Me_3 represents three methyl structures. $\text{C}_n[M]$ unambiguously represents the structures, where n is the number of carbon atoms and N is the number of monomer units.

FIG. 3. Resonance integrals used for PDA with bond alteration in the l th unit cell. t_s is the resonance integral for the single, t_t for the triple, and t_d is for the double bond. The periodicity of polydiacetylene is given by $4a$, where a is the undimerized bond length.

FIG. 4. Schematic energy band structure of polydiacetylene in the reduced Brillouin zone for the acetylene structure. E'_g is the energy gap within the valence bands. E_g is the energy gap between the upper valence band and the conduction band. Numerical estimates are from the parameters of Table 2.0 (see text).

FIG. 5. The four essential states.

FIG. 6. Excitation energies for the $1B_u$, $2A_g$, mA_g and nB_u states for the PPP model as function of the inverse of the number of carbon atoms, $1/n$. The $1B_u$ experimental excitation

energies are included for comparison.

FIG. 7. The states contributing to the non-linear properties of PDA and the important one-photon transitions between them. The dipole moments are shown for a chain of 26 atoms.

FIG. 8. Particle-hole separation for the $1B_u$, $2A_g$, mA_g and nB_u states in units of the average C-C distance as a function of the number of the number of carbon atoms, n .

		R	d(C≡C)	D(C=C)	D(C-C)	sp^2 angle ^a
	PTS-6	<i>b</i>	1.191	1.356	1.428	121.9
PDAs	P-MBS	<i>c</i>	1.195	1.364	1.424	-
	P-THD	<i>d</i>	1.205	1.426	1.359	119.1
PDAs used in this paper	C₁₄[3]	H	1.202	1.329	1.427	123.0
	C₂₂[5]	H	1.208	1.360	1.412	122.9

^a bond angles in degrees between an sp^2 carbon atom and the next sp atom.

b R=-CH₂-OTos at 295 K.

c R=-CH₂-SO₃-Ph-*p*OMe at 295 K.

d R=-CH₂-N(Ph)₂ at 295 K.

Table 1.

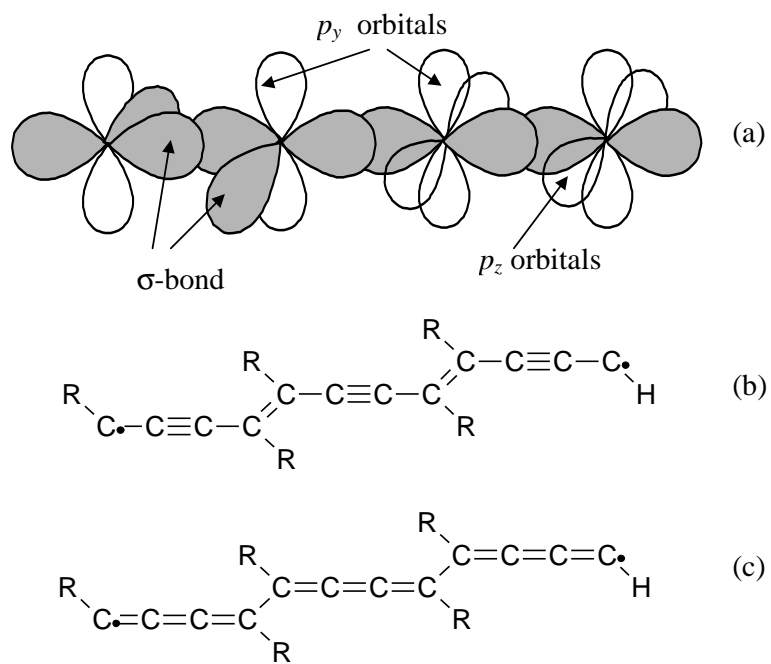


Fig. 1.

t_0	2.539 eV
α	4.593 eV/Å
r_0	1.4 Å
U	10.06 eV
t_s	2.4494 eV
t_d	2.7939 eV
t_t	3.4346 eV

Table 2.

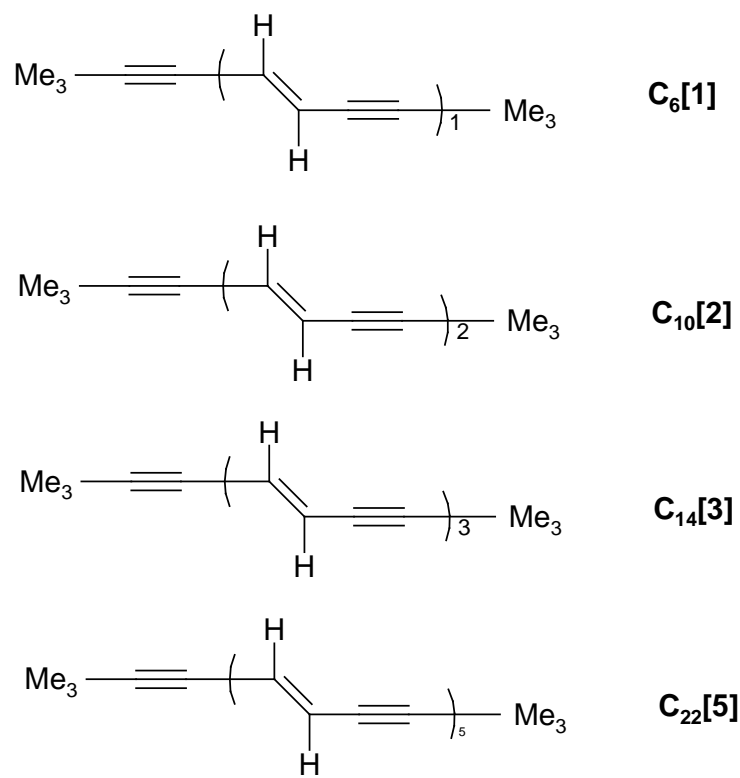


Fig. 2.

Chain Length		1Ag - 1Bu		1Bu - mAg		mAg - nBu	
n	N	Dipole Moment	ΔE	Dipole Moment	ΔE	Dipole Moment	ΔE
6	1	1.5125	5.1633	2.2657	8.8850	2.5579	14.0138
10	2	2.1523	4.3072	2.3221	7.5846	2.7554	10.5006
14	3	2.6615	3.8860	3.9430	6.6115	4.7893	9.0628
18	4	3.0926	3.6483	4.5245	6.1595	5.4395	8.2927
22	5	3.4679	3.5015	3.4514	5.8547	4.1472	7.8628
26	6	3.8018	3.4049	3.5629	5.6994	3.8258	7.5910

Table 3.

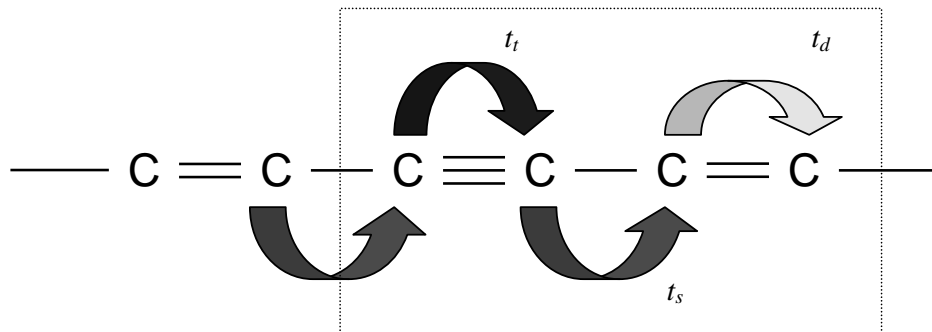


Fig. 3.

State	E_{∞} (eV)
$1B_u$ Theory	3.021
Exp.	2.5113
Charge gap, Δ	5.7351

Table 4.

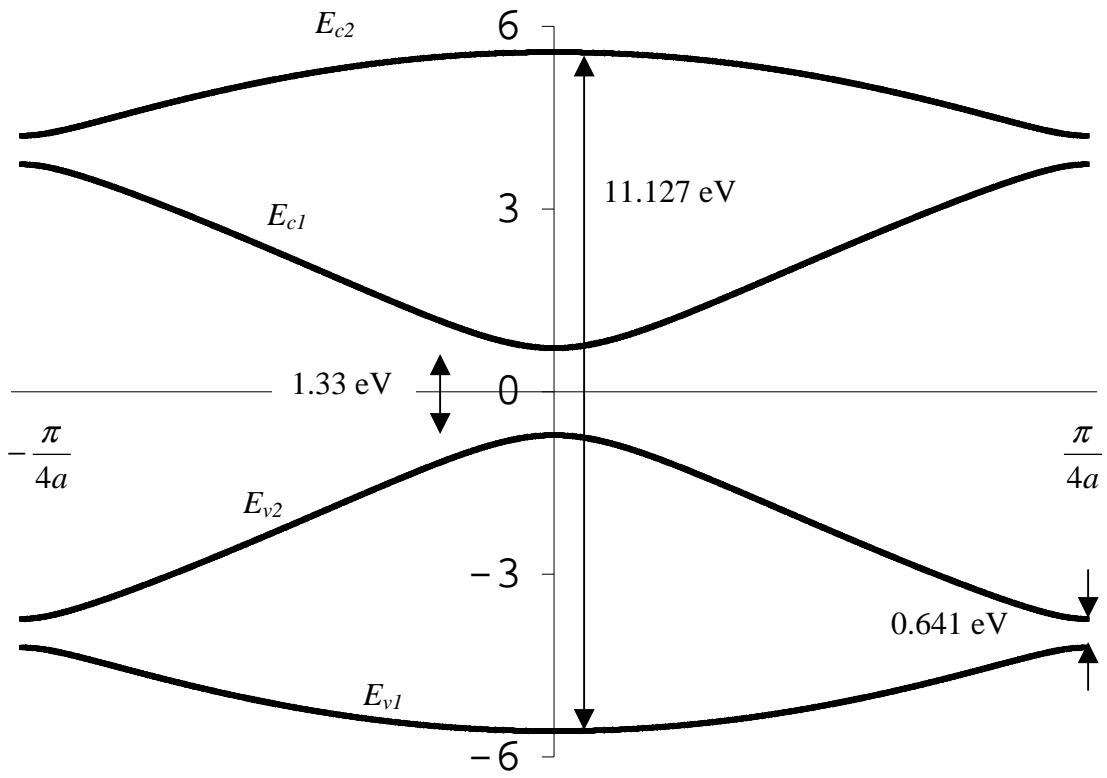


Figure 4

Essential States

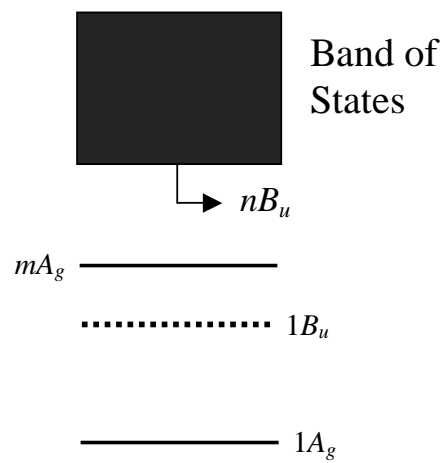


Fig. 5.

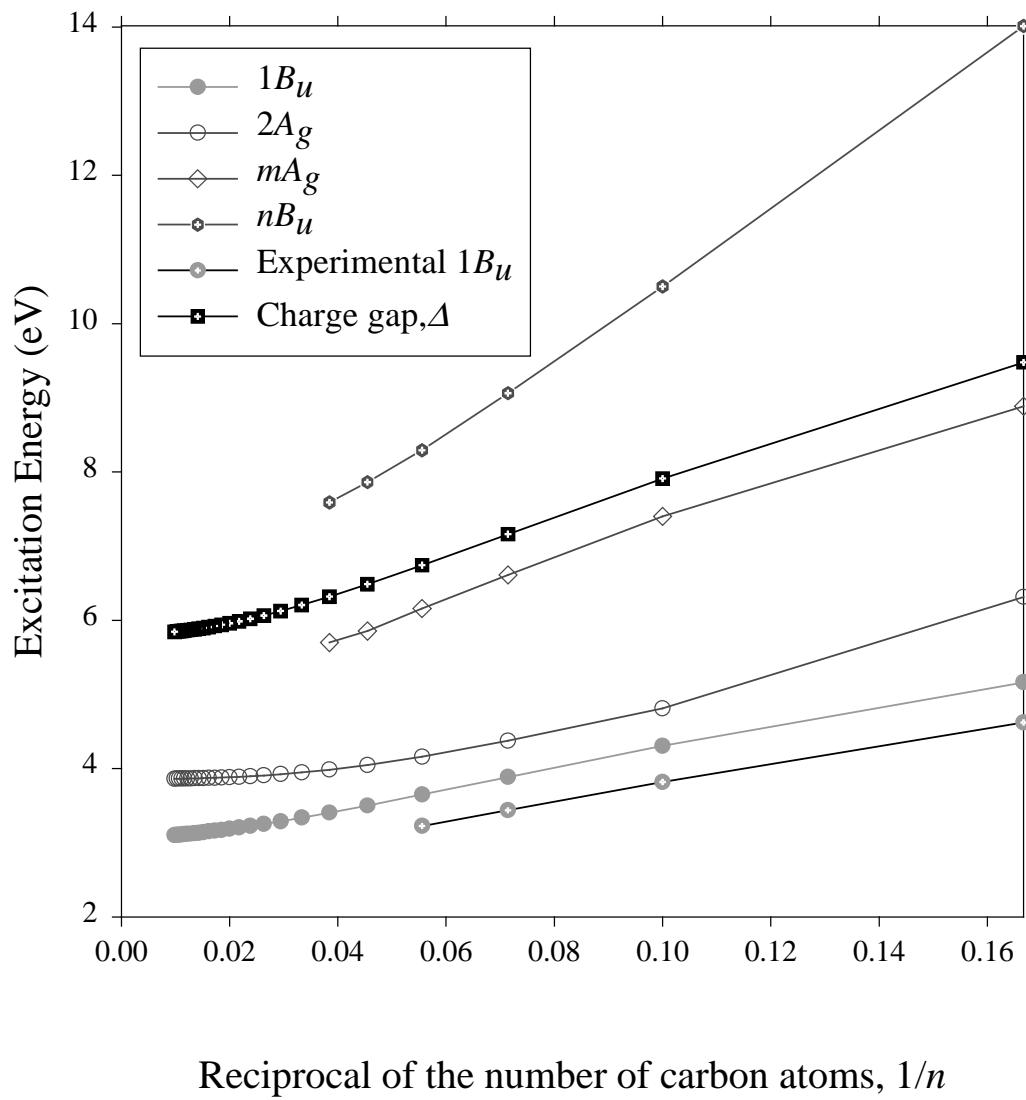


Fig. 6.

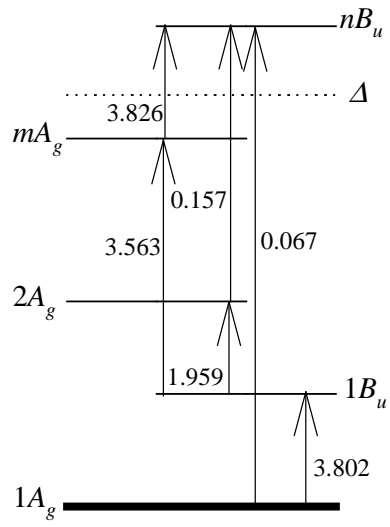


Fig. 7

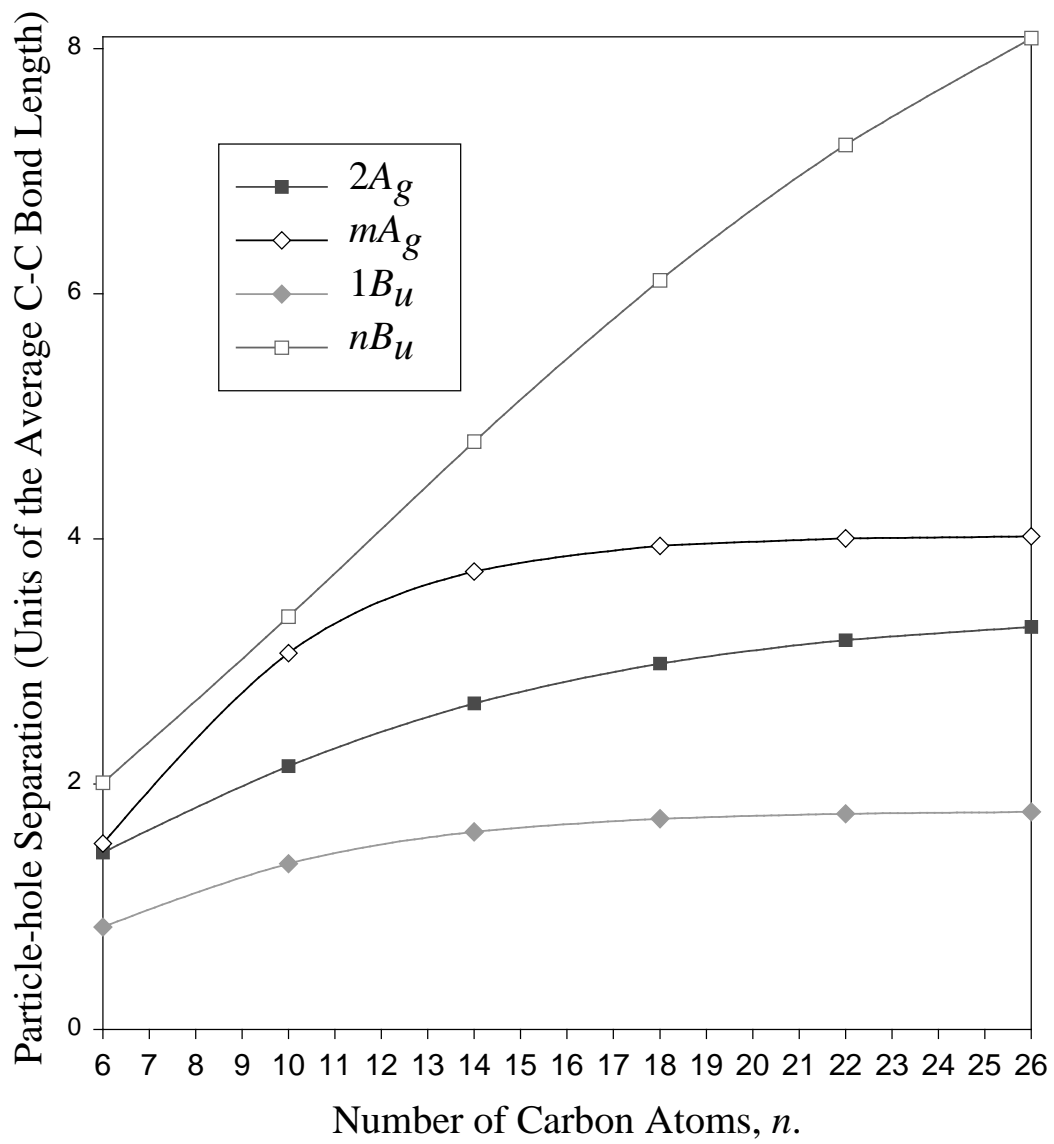


Fig. 8.